GeroScience (2022) 44:1457–1477
https://doi.org/10.1007/s11357-022-00534-2

ORIGINAL ARTICLE

Long-term exercise pre-training attenuates Alzheimer's disease–related pathology in a transgenic rat model of Alzheimer's disease

Luodan Yang · Chongyun Wu · Yong Li · Yan Dong · Celeste Yin-Chieh Wu · Reggie Hui-Chao Lee · Darrell W. Brann · Hung Wen Lin · Quanguang Zhang

Received: 3 January 2022 / Accepted: 17 February 2022 / Published online: 28 February 2022

Abstract Alzheimer's disease (AD) is the most common form of dementia. Despite enormous efforts around the world, there remains no effective cure for AD. This study was performed to investigate the effects of long-term exercise pretreatment on the typical pathology of AD in a novel transgenic AD rat model. Male 2-month-old animals were divided into the following groups: wild-type (WT) rats, AD rats, and AD rats with treadmill exercise pretreatment (AD-Exe). After exercise pretreatment, the Barnes maze task, passive avoidance task, and cued fear conditioning test were performed to test learning and memory function. The elevated plus maze, open field test, sucrose preference test, and forced swim test were conducted to measure anxious-depressive–like behavior. Immunofluorescence staining, Golgi staining, transmission electron microscopy, Western blot analysis, F-Jade C staining, TUNEL staining, and related assay kits were conducted to measure Aβ plaques, tau hyperphosphorylation, neuronal damage, neuronal degeneration, dendritic spine density, synapses, synaptic vesicles, mitochondrial morphology, mitochondrial dynamic, oxidative stress, and neuroinflammation. Behavioral tests revealed that long-term exercise pretreatment significantly alleviated learning and memory dysfunction and anxious-depressive–like behaviors in AD animals. In addition, exercise pretreatment attenuated amyloid-β deposition and tau hyperphosphorylation and preserved spine density, synapses, and presynaptic vesicles. Exercise also inhibited neuronal damage, neuronal apoptosis, and neuronal degeneration. Additional studies revealed the imbalance of mitochondrial dynamics was significantly inhibited by exercise pretreatment accompanied by a remarkable suppression of oxidative stress and neuroinflammation. Our findings suggest that long-term exercise pretreatment alleviated behavioral deficits and typical pathologies of the AD rat model, supporting long-term exercise pretreatment as a potential approach to delay the progression of AD.

Keywords Treadmill exercise · Alzheimer's disease · Amyloid-β deposition · Mitochondrial dynamics · TgF344-AD rats · Memory

Luodan Yang and Chongyun Wu contributed equally to this work.

L. Yang · C. Y.-C. Wu · R. H.-C. Lee · H. W. Lin · Q. Zhang (✉)
Department of Neurology, Louisiana State University Health Sciences Center, 1501 Kings Highway, Shreveport, LA 71103, USA
e-mail: qzh001@lsuhs.edu

L. Yang · C. Wu · Y. Li · Y. Dong · D. W. Brann
Department of Neuroscience and Regenerative Medicine, Medical College of Georgia, Augusta University, 1120 15th Street, Augusta, GA 30912, USA

Introduction

Alzheimer's disease (AD), an irreversible, progressive brain disease, is the most common form of dementia

and is clinically characterized by progressive cognitive deficits, neurofibrillary tangles (NFTs), and amyloid plaques [1–3]. As the fifth leading cause of death for adults aged 65 years and older in the USA [4], AD exerts a high health, socioeconomic, and emotional burden to both society and patients [5]. Although many long and expensive clinical trials have been conducted, there is currently no cure for AD [6].

The failure of clinical trials to yield effective new therapies for AD has led many to reconsider the amyloid and tau hypotheses, which have been the cornerstone for much of AD research conducted in the past decades [2, 7]. In fact, a growing body of research supports AD as being a multifactorial disease caused by multiple etiological factors involving numerous genes, environmental factors, or the interactions between them [8, 9]. Therefore, studies targeting one etiological factor or single pathway may not slow down or reverse the progression of AD [9]. In addition, inappropriate AD animal models may impede the successful translation of findings to clinical trials [10]. As reported in previous studies, most mouse AD models cannot mimic all the features of AD without additional human transgenes that are not related to familial AD [10–12]. Furthermore, the use of an inappropriate therapeutic time window has been considered as another reason for the failure of many clinical trials[10]. It is widely accepted that AD is an irreversible brain disorder, and it would be difficult for a treatment performed after neuronal and synaptic loss to improve learning and memory abilities [13–16]. Therefore, increasing research has focused on AD prevention and interventions before the brain undergoes irreversible damage [3, 5, 17–19].

In an attempt to address these concerns and shortcomings, this study focused on the effects of exercise, a nonpharmacological treatment that targets multiple factors and pathways. In addition, we used a novel AD rat model of familial AD with all the typical features of human AD, including amyloid plaques, NFTs, synapse loss, neuronal loss, neuronal degeneration, gliosis, and cognitive impairment [5, 12]. Notably, the present study was conducted to analyze the effects of long-term exercise pretreatment on AD before pathological features were detected rather than post-treatment. Taken together, the current study was designed to investigate the effect of exercise pretreatment on multiple AD pathologies using a novel AD rat model with the hope of providing more evidence for the preventive effect of exercise.

Materials and methods

Animals

TgF344-AD rats and wild-type rats (2 months old) were used in the current study. AD rats were originally genetically engineered at Emory University [12]. Rat genotyping was performed to distinguish the transgene-negative rats from transgene-positive rats following our previously published procedures [5]. The wild-type rats had the same genetic background hybrid as TgF344 rats. Male experimental animals were randomly divided into the following three groups: (1) WT rats ($n = 12$), (2) AD rats ($n = 12$), and (3) AD rats with long-term exercise training (AD-Exe, $n = 13$). All animals used in this study were housed in standard caging with ad libitum access to food and water. Animal environment, housing, management, and other procedures were approved by our Institutional Animal Care and Use Committee (IACUC) of Augusta University and complied with National Institutes of Health guidelines.

Treadmill exercise

As reported in our previous study [5], 8 months of treadmill exercise training initiated at 2 months old and ended at 10 months old. The treadmill exercise training included a 2-week adaptive training stage followed by an exercise training stage. The adaptive training stage was initiated at 4 m/min for 15 min and then 6 m/min for 30 min, 8 m/min for 45 min, 12 m/min for 45 min, and finally 18 m/min for 45 min. During the following exercise training stage, exercise training was performed with constant intensity at 18 m/min for 45 min three times a week from the 3rd week of training until the rats were 10 months old. The behavioral tests were performed at 18 months of age following by 8 months of detraining.

Behavioral tests

Barnes maze task

The Barnes maze is a well-established behavioral test to assess spatial learning and memory in rodents [20]. As described by our group previously, this behavioral task consists of 3 days of training trials

and a probe trial [3]. During the 3-day training trial, animals were given a maximum of 3 min to explore freely, and an overhead video camera connected with ANY-maze video tracking software (Stoelting, Wood Dale, IL, USA) was used to record the motion traces of the animals. The latency to find the hidden chamber beneath a target hole and the total number of errors were recorded and analyzed. The hidden chamber was removed on the probe day, and the target hole was blocked with a small black plastic board. The time the animal spent in the target zone where the target hole was previously located and the numbers of target zone entries were recorded during the 90-s probe trial.

Passive avoidance task

The passive avoidance task is a fear-motivated test commonly used to measure learning and memory in rodents [5, 21]. The apparatus used for the passive avoidance task is divided into a lit compartment (white and illuminated by a 24 V–10 W bulb) and a dark compartment with a gate between them. During the 5-min acquisition/conditioning phase (training phase), the rat is placed in the lit compartment and allowed to explore both compartments freely. During this stage, after the rat enters the dark compartment, the rat was given a 2-s mild foot shock with the gate closed. On the following day (test phase), the rat was placed back in the lit compartment similar to the training phase but without electric foot shock in the dark compartment. The latency from the lit compartment to the dark compartment was recorded and analyzed by ANY-maze tracking software.

Cued fear conditioning test

The cued memory test is a fear-based learning task to assess associative fear learning and memory in rodents [22]. The apparatus used for the cued fear conditioning task includes a chamber to deliver a mild electric foot shock and a totally different chamber without foot shock. During the conditioning phase, rats were placed in the conditioning chamber for 6 min, and 2-s foot shocks were given at the end of every 2 min with a 30-s tone before the foot shock. On the cued test day, the rats were placed in another chamber similar to the conditioning phase but without electric foot shock after 30-s tones. The total freezing time was recorded and analyzed by ANY-maze tracking software.

Elevated plus maze

The elevated plus maze is a widely used behavioral assay to detect anxiety-like behavior in rodents [5, 23]. A plus-shaped apparatus elevated 50 cm above the floor with two opposite closed arms opposite to two open arms were used for the test. During the test, rats were placed on the central platform and given a maximum of 5 min to explore the apparatus. The animal's total time in the open arms, movement tracking plot, and the total number of open arm entries were recorded and quantified using ANY-maze software.

Open field test

The open field test is a widely used test to assess anxiety-related behavior, activity, and exploratory behavior in rodents [5, 24]. The apparatus used in the test is a wall-enclosed area (56 cm × 56 cm) surrounded by 50-cm-tall walls. The enclosed black area is marked with square grid lines. During the test, the rats were placed at the corner of the apparatus and given a maximum of 5 min to explore the field freely. The number of line crossings, motion tracking plot, and defecations in the open field were recorded and analyzed.

Sucrose preference test

The sucrose preference test is a widely used behavioral task used to investigate depression-like behavior based on rats' natural preference for sweets [25]. It was performed as described previously by our group [5]. Prior to beginning testing, rats were habituated with two bottles of plain water for 2 days, followed by 2% sucrose solution for another 2 days in their home cage. Thereafter, the rats were deprived of water and sucrose solution for 24 h. On the testing day, animals were singly housed in their home cage with ad libitum access to the 2% sucrose solution and plain water for 8 h. Sucrose and water intake were calculated on an absolute basis. Sucrose preference was calculated using the following formula: Preference = (sucrose intake/ (water intake + sucrose intake)) × 100%.

Forced swim test

The forced swim test is a widely used rodent behavioral test to investigate depressive-like behavior [5].

Rats were allowed to swim in a plastic cylinder filled with 30-cm-deep water at 23–25 °C for 6 min. Immobility time (no noticeable movement more than 1 s) was recorded by ANY-maze video tracking system.

Brain collection and tissue preparation

The brains were collected at 18 months of age following behavioral tests. As described in our previous study [26], the rat brains were quickly removed under deep anesthesia following transcardial perfusion with ice-cold saline. One side of the brain was post-fixed with 4% paraformaldehyde (PFA) and then cryoprotected with 30% sucrose solution. The hippocampus and cortex were quickly dissected from the remaining hemisphere and frozen using liquid nitrogen. Brain sections were prepared using a Leica Rm2155 microtome (25 μm each) and stored in stock solution (FD NeuroTechnologies, Inc., Columbia, MD, USA; Catalog number: PC101) until future analysis. For the preparation of the protein sample, the frozen samples stored at − 80° were homogenized in ice-cold homogenization buffer (50-mM 4-(2-hydroxyethyl)-1-piperazineethanesulfonic acid [HEPES], 12-mM β-glycerophosphate, 150-mM NaCl, 1% Triton X-10, protease, and phosphatase inhibitors) using a motor-driven Teflon homogenizer. Total protein fractions and mitochondrial protein fractions from the cortex and hippocampus were measured using a Modified Lowry Protein Assay kit (Pierce, Rockford, IL, USA) as described in our previous study [27].

Spine density analysis

Golgi staining was carried out to examine the changes in spine density according to the manufacturer's protocol (FD Rapid GolgiStain™ kit, FD NeuroTechnologies, Inc.). In brief, rat brains were quickly removed under deep anesthesia without perfusion. Thereafter, the brains were immersed in a pre-prepared impregnation solution and stored at room temperature for 14 days in the dark. The brains were subsequently transferred into a manufacturer-provided solution C and stored at room temperature for 96 h. A 200-μm-thick coronal whole-brain sections were mounted with solution C on gelatin-coated slides and allowed to dry naturally at room temperature for 2 days. After washes with distilled water, the brain sections were then incubated with a mixture consisting of manufacturer-provided solution D and E for 10 min. After washes, brain sections were subsequently dehydrated and cleared with ethanol and xylene. An OLYMPUS IX70 microscope was used to capture the images at 100 × total magnification. Spine dendrites were processed and analyzed using ImageJ software. For the spine density analysis, spine densities from five individual neurons in both cortex and hippocampus were measured. The spine density analysis measured spine densities from five individual neurons in both the cortex and hippocampus. Three to four brain slices were randomly chosen and analyzed for each animal and presented as a single value for each brain slice. For each group, four animals were included in the spine density analysis. The experimenters were blind in conducting data analysis in all the tests.

Transmission electron microscopy

Rat brains were quickly removed under deep isoflurane anesthesia followed by post-fixation in 2% glutaraldehyde and 2% paraformaldehyde for 2 h at 4 ℃. After three washes with phosphate buffer, the brains were post-fixed with 1% osmium tetroxide for another 2 h and washed in phosphate buffer three times. After dehydration in ethanol and propylene oxide series, the brain tissues were then embedded in EmBed812. Ultrathin Sects. (70 nm) were collected and treated with uranyl acetate and lead citrate. Images from low magnification to high magnification were visualized and captured using a JEM 1230 transmission electron microscope (JEOL USA Inc., Peabody, MA) at 110 kV with an UltraScan 4000 CCD camera. Six to eight brain slices were randomly chosen and analyzed for each animal, with the mean value presented as a single value for each animal. For each group, four animals were included in the analysis.

Immunofluorescence staining

Immunofluorescence staining was performed as previously described by our group [28]. Briefly, brain sections were permeabilized with 0.4% Triton X-100 and blocked with 10% normal donkey serum for 1 h. Thereafter, the sections were incubated with primary antibodies for 24 h at 4 °C. The primary antibodies used in this study include the following: anti-4G8 β-amyloid antibody (BioLegend; San Diego, CA, USA); anti-PHF1

(Thermo Scientific; Rockford, IL, USA;), anti-Iba-1 (Wako Chemicals; Richmond); anti-8-OHdG and PGC-1α (Abcam; Cambridge, MA, USA), anti-GFAP, MAP2 (Thermo Fisher Scientific, Waltham, MA, USA); anti- NeuN, MBP, Mfn1, Fis1, and Tom20 (Proteintech, Rosemont, IL, USA); anti-SOD2 (Santa Cruz Biotechnology; Dallas, TX, USA). After three washes, the brain sections were incubated with Alexa Fluor donkey anti-goat/mouse/rabbit secondary antibodies (594/647/488, Thermo Fisher Scientific) for 1 h at room temperature. After washes with 0.1% Triton X-100 solution, the brain sections were mounted and coverslipped using DAPI Fluoromount-G (SouthernBiotech; Birmingham, AL, USA). Confocal images of Tom 20 staining were processed by ImageJ software according to our previous protocol [29]. For the immunofluorescence staining, 3–4 brain slices with intact hippocampal subfields were randomly chosen from each rat. Each brain slice's fluorescence intensity was averaged to provide a single value for each rat. Furthermore, all the images were acquired under the same image acquisition parameters. Quantification of microglia morphology was performed according to a previous study [30].

Western blotting analysis

Western blotting analysis was performed following the procedure described in previous studies [31, 32]. In brief, the protein samples were separated based on molecular weight using an electrophoresis apparatus (Bio-Rad, Hercules, CA, USA) with 4–20% sodium dodecyl sulfate–polyacrylamide gel (SDS) and transferred onto polyvinylidene difluoride (PVDF) membrane. After blocking, the PVDF membranes were then incubated with the following antibodies overnight at 4 °C: anti-PGC-1α (Abcam; Cambridge, MA, USA), anti- Mfn1, Fis1, and COX4 (Proteintech, Rosemont, IL, USA); anti-SOD2 (Santa Cruz Biotechnology; Dallas, TX, USA). After washing, the PVDF membranes were then incubated with appropriate Horseradish Peroxidase (HRP)–conjugated secondary antibodies for 1 h at room temperature. Thereafter, the images of bound protein were captured by a cold CCD digital imaging system followed by semi-quantitative analyses using ImageJ software (Version 1.49, NIH). GAPDH and COX4 were used as a loading control. The intensity of the target bands was normalized to the corresponding loading controls and expressed as a percentage of the WT group.

TUNEL and F-Jade C staining

TUNEL and Fluoro-Jade C (F-Jade C) staining were carried out to test cellular apoptosis and neuronal degeneration as previously described [20, 28]. The apoptotic cells in the cortex and hippocampus were detected using a Click-iT® Plus TUNEL assay kit (Thermo Fisher Scientific) according to the manufacturer's protocol. F-Jade C staining was utilized to detect neuronal degeneration. Brain sections were incubated with F-Jade C (Sigma-Aldrich, St. Louis, MO, USA) working solution for 20 min according to the manufacturer's protocol. After washes, the brain sections were mounted using DAPI Fluoromount-G (Southern Biotech; Birmingham, AL, USA). Images of the brain sections were captured using LSM700 Meta confocal laser scanning microscope (Carl Zeiss).

Total antioxidant capacity assay

The total antioxidant capacity of protein samples from the cortex and hippocampus were determined by an antioxidant assay kit (709,001; Cayman Chemical; Ann Arbor, MI, USA) [3, 5]. In brief, 20 µg of protein samples were mixed with chromogen (150 µl) and metmyoglobin (10 µl) in the designated wells provided in the antioxidant assay kit. The working solution (40 µl of hydrogen peroxide) was added to the well and incubated for 5 min. Thereafter, the absorbance of each sample was measured on a spectrophotometer at 750 nm. A Trolox standard curve was used to calculate the antioxidant capacity of each sample. Data was expressed as percentage changes compared to the WT group.

Protein carbonyls determination

Protein carbonyls in the cortex and hippocampus were determined using a Protein Carbonyl Colorimetric Assay Kit (Cayman Chemical, Ann Arbor, MI, USA) as described in our previous studies [3, 5]. Briefly, 20 µg of protein from each sample was denatured using 12% SDS and incubated with 1X DNPH solution for 15 min at room temperature. Thereafter, protein samples were mixed with neutralization solution (7.5 µl) and then loaded in PVC ELISA microtiter plate. The levels of protein carbonyls were measured

by ELISA analysis. The absorbance of each sample was measured on a plate reader at 370 nm.

Lipid peroxidation (MDA) assay

The malondialdehyde production in the cortex and hippocampus was measured using a lipid peroxidation (MDA) assay kit (Abcam, Cambridge, UK) following the manufacturer's protocol. Briefly, protein samples (200 µl) were incubated with TBA reagent (600 µl) at 95 °C for 60 min. After incubation, the samples were cooled to room temperature in an ice bath for 10 min. Thereafter, 200 µL of supernatant (containing MDA-TBA adduct) was moved into a 96-well microplate and then measured at 532 nm on a microplate reader for colorimetric assay. Results were expressed as percentage changes compared to the WT group.

Proteome profiler rat cytokine analysis

Levels of inflammatory cytokines were measured using a Proteome Profiler Rat Cytokine Array Kit (R&D Systems, Inc., MN, USA) as previously described [26]. In brief, 800 µg of protein samples from the cortex and hippocampus were mixed with a reconstituted detection antibody cocktail and incubated with the membrane provided in the assay kit. After washes, 2 mL of diluted streptavidin-HRP were incubated with the membrane for 30 min at room temperature. The images of protein in the membrane were captured by a cold CCD digital imaging system. The density of dots was analyzed by ImageJ software (Version 1.49, NIH). The acquired data was calculated as *z*-scores and expressed as a heat map using R package (R i386 3.6.2. lik). The fold change was calculated as the ratio of the difference between AD and WT group or AD-Exe and WT group. Log2 fold change was calculated as Log2(fold change) to compare among groups for statistical differences.

Statistical analysis

SigmaStat (Systat Software; San Jose, CA, USA) were used to analyze all the data. One-way analysis of variance (ANOVA) followed by Student–Newman–Keuls (S–N-K) post hoc tests were applied for all dependent variables between groups. Two-way (group*time) repeated measures of ANOVAs followed by Tukey's all pairwise comparisons test was applied for variables with multiple time points. All data were expressed as the mean ± SEM. For all test, P values < 0.05 were considered significant.

Results

Long-term exercise training attenuates Aβ accumulation and tau hyperphosphorylation in TgF344-AD rats

Aβ accumulation and tau hyperphosphorylation are hallmarks of AD [33]. Therefore, we first investigated the role of exercise pretreatment on Aβ accumulation and tau hyperphosphorylation using staining of cortical and hippocampal sections for 4G8, a marker of amyloid deposition, and PHF for hyperphosphorylated tau. As shown in Fig. 1A, 4G8 staining revealed that both the cortex and hippocampus from AD animals exhibit substantial amyloid deposition, which was significantly attenuated in the exercise pretreatment group. As shown in Fig. 1B, AD animals also exhibited abnormal tau hyperphosphorylation, as evidenced by increased phosphorylation of tau protein (PHF) fluorescent intensity in the cortex and hippocampus, an effect that was significantly abated by long-term exercise training.

Long-term exercise training attenuates memory impairment and anxious-depressive–like behavior of TgF344-AD rats

We next investigated the effect of long-term treadmill exercise training on cognitive function and anxious-depressive–like behaviors in 18-month-old AD rats using a battery of behavioral tests. As shown in Fig. 2A, the Barnes maze was utilized to measure spatial learning and memory. On the second and third day of training trials, AD animals displayed a longer escape latency compared with WT animals, suggesting that 18-month-old AD animals exhibit impaired learning and memory abilities. In contrast, the learning and memory impairments in AD animals were significantly ameliorated by long-term exercise training, as evidenced by significantly decreased escape latency on the second and third days of the training trials. Furthermore, AD animals exhibited significantly increased exploration errors before finding the hidden box compared to WT animals, which

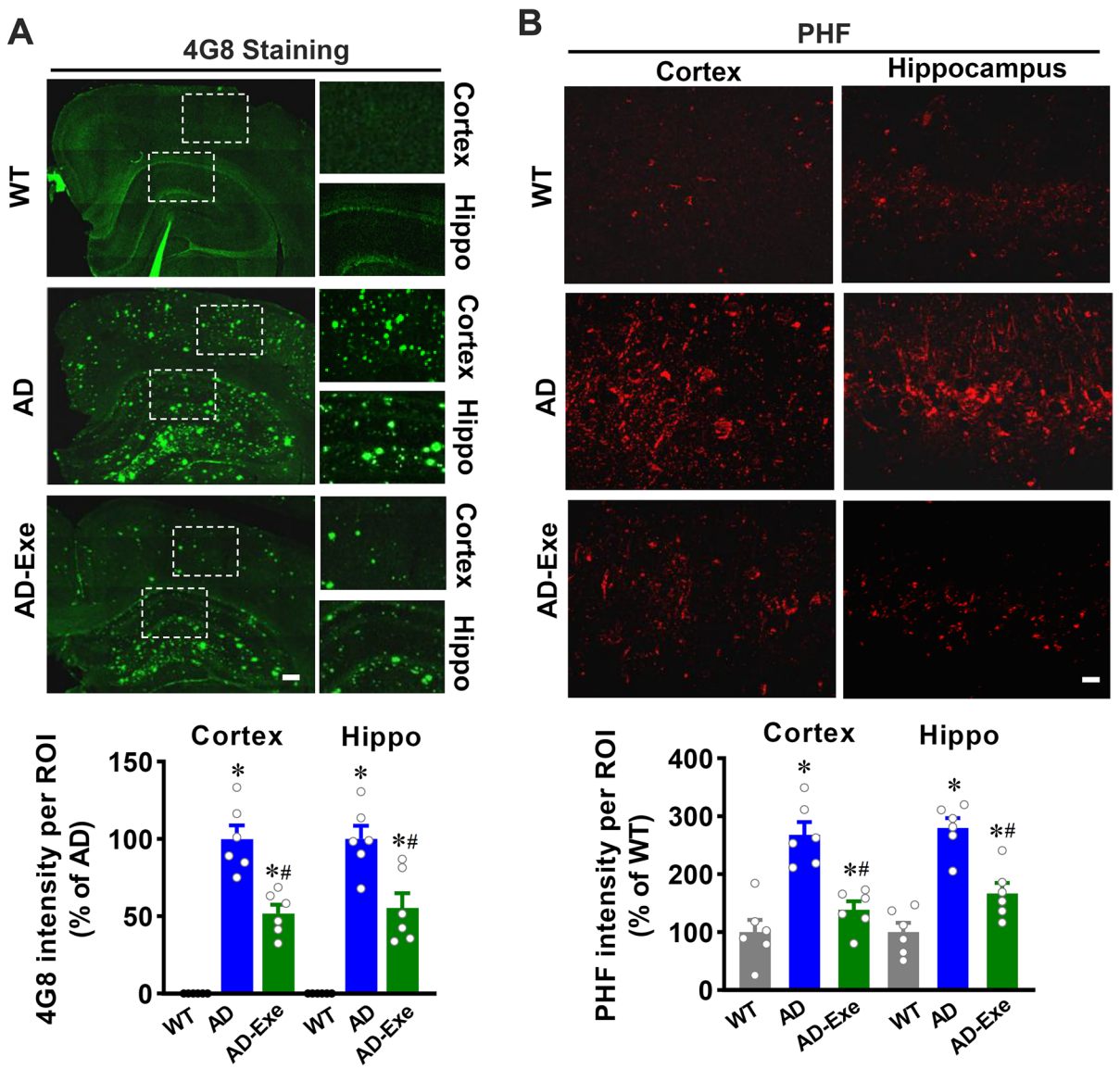

Fig. 1 Long-term exercise training attenuates Aβ accumulation and tau hyperphosphorylation in TgF344-AD rats. **A** Representative confocal microscopy images of Aβ accumulation using Aβ 4G8 antibody. Scale bar = 200 μm. **B** Representative confocal microscopy images of phosphorylation of tau protein (PHF). Scale bar = 10 μm. All data are expressed as mean ± SEM ($n = 6$). *$P < 0.05$ versus WT group, #$P < 0.05$ versus AD group

was notably decreased in the exercise training group. During the probe trial, the quadrant occupancy and the number of field entries significantly decreased in AD animals (AD vs. WT). However, AD animals in the exercise group showed increased quadrant occupancy and field entries (AD vs. AD-Exe).

The passive avoidance test and cued memory test were also performed to assess learning and memory based on negative reinforcement. As shown in Fig. 2B, there were no significant differences among the three groups in the latency of entrance to the dark boxes during the acquisition phase, suggesting they were at the same level before the electrical shock. Intriguingly, during the test phase, both WT and AD animals in the exercise group displayed significantly increased latency to enter the dark box

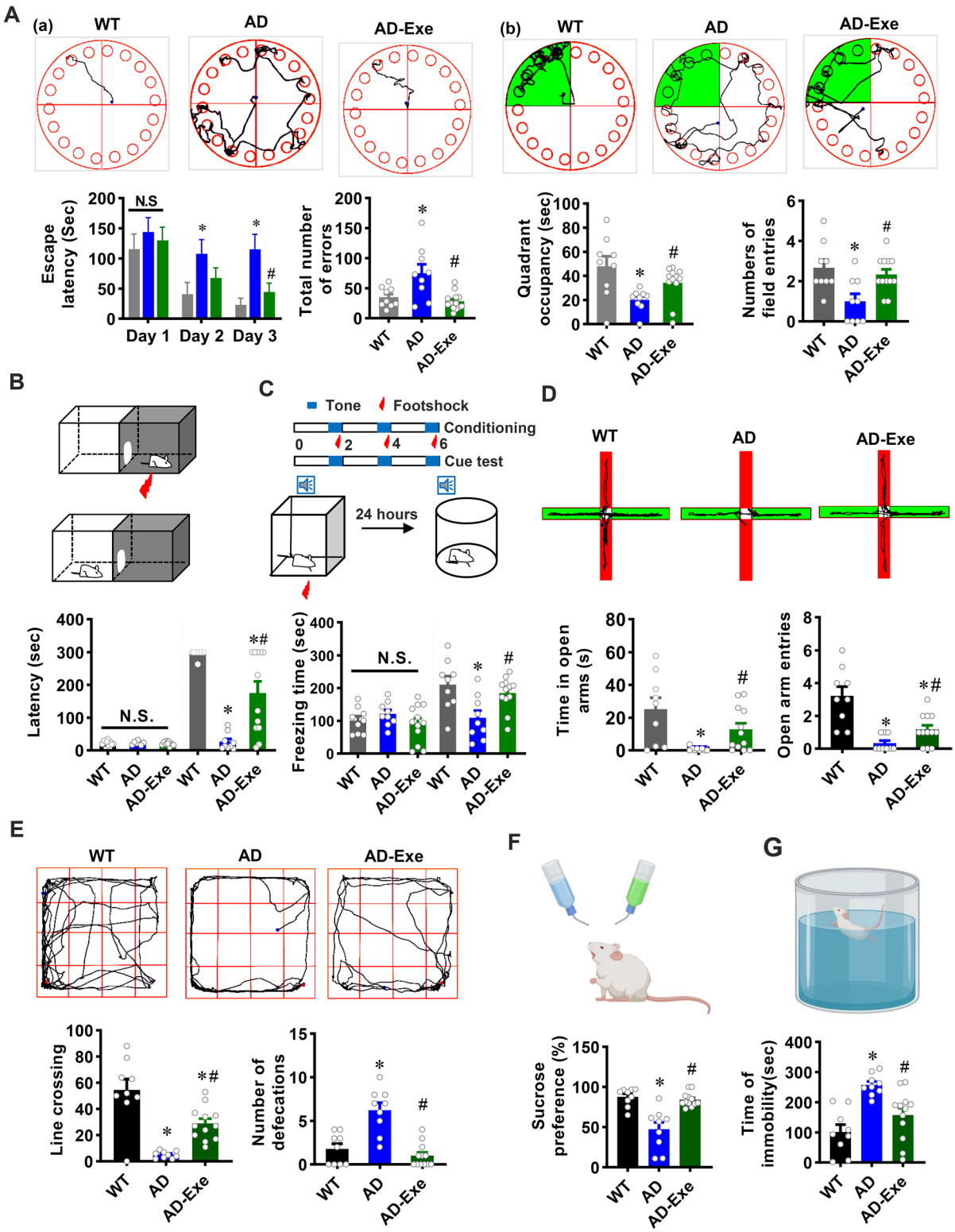
A
(a)
WT
AD
AD-Exe
(b)
WT
AD
AD-Exe
Escape latency (Sec)
N.S
Day 1
Day 2
Day 3
Total number of errors
Quadrant occupancy (sec)
Numbers of field entries
B
C
Tone
Footshock
Conditioning
Cue test
24 hours
D
Latency (sec)
N.S.
Freezing time (sec)
Time in open arms (s)
Open arm entries
E
Line crossing
Number of defecations
F
Sucrose preference (%)
G
Time of immobility(sec)

◂**Fig. 2** Long-term exercise training attenuates memory impairment and anxious-depressive–like behavior of TgF344-AD rats. **A** The Barnes maze task was performed to measure learning and memory function. (a) Representative tracking plots of rats and results of escape latency and the total number of errors before finding the target box on the training days. (b) Representative tracking plots of rats and results of quadrant occupancy and number of field entries on probe trial day. **B** The passive avoidance task was conducted to test fear memory. Latency from the lit compartment to the dark compartment. **C** Cued fear conditioning test was performed to assess associative fear learning and memory. Freezing times were recorded and analyzed. **D** The elevated plus maze was performed to detect anxiety-like behavior. The time each rat stayed in the open arms and the entries to the open arms were analyzed. **E** The open field test was performed to assess anxiety-related behavior. Line crossing and defecations in the open field were recorded and analyzed. **F** The sucrose preference test and **G** forced swimming test were performed to measure depressive-like behavior. All data are expressed as mean ± SEM ($n = 9–12$). $^{*}P < 0.05$ versus WT group, $^{\#}P < 0.05$ versus AD group

as compared with AD animals, which suggests that exercise training significantly alleviated fear memory in AD animals. Furthermore, cued memory was impaired in AD animals, as evidenced by significantly decreased freezing time compared with WT, which was significantly attenuated by long-term exercise training (Fig. 2C). Taken together, our results show that long-term exercise training is capable of attenuating learning and memory impairment in AD rats.

Next, the elevated plus maze, open field test, sucrose preference test, and forced swim test were utilized to measure the anxious-depressive–like behavior of TgF344-AD rats. As shown in Fig. 2D, AD rats displayed significantly decreased time and total entries (AD vs. WT) in the open arms of the elevated plus maze, which was ameliorated by long-term exercise training. Furthermore, in the open field test (Fig. 2E), the number of line crossings was significantly decreased in the AD group as compared to animals from the WT group and the long-term exercise group. However, the number of defecations in the open field after each test was significantly increased in the AD group but was attenuated substantially in the long-term exercise training group. Additionally, as shown in Fig. 2F, AD animals exhibited a significantly decreased preference for sucrose as compared to both WT animals and exercise, suggesting AD animals had depression-like behaviors that were alleviated by long-term exercise training. The forced swim test further confirmed the development of depression-like behaviors in AD animals and the blunting of these changes in long-term exercise-treated AD animals, as evidenced by increased immobility of AD animals (AD vs. WT) and significantly decreased immobility of long-term exercise-treated AD animals (AD vs. Exe, Fig. 2G). These data indicate that long-term exercise pretreatment significantly attenuates anxious-depressive–like behavior of AD rats.

Long-term exercise training preserves dendritic spine density, synapses, and synaptic vesicles of TgF344-AD rats

It is known that functional deficits are closely related to the structural alterations of the synapse and dendritic spine density. Therefore, we next explored the effect of exercise training on dendritic spine density, synaptic vesicles, and synapses of AD rats. As shown in Fig. 3A, apical dendritic spine density in CA1 region and cortex were selected for analysis. The results of Golgi staining revealed that the spine density in both the cortex and hippocampus was significantly decreased in AD animals as compared with WT animals. Intriguingly, the decrease of spine density in the cortex and hippocampus of AD rats could be significantly preserved by long-term exercise training. In line with this finding, the numbers of synapses and vesicles per bouton were significantly decreased in AD animals (Fig. 3B, AD vs. WT). However, AD animals with long-term exercise pretreatment showed decreased synaptic loss and preserved synaptic vesicles in the presynaptic terminal.

Long-term exercise training alleviates neuronal damage, apoptosis, and degeneration in TgF344-AD rats

Abnormal Aβ accumulation and tau hyperphosphorylation could result in neuronal damage, apoptosis, and degeneration in AD, according to previous studies [3, 34]. Therefore, we next investigated the effect of long-term exercise training on neuronal damage, apoptosis, and degeneration. MAP2 is an early and sensitive marker for neuronal damage. As shown in Fig. 4A, representative confocal microscopy images of MAP2 staining revealed that AD animals displayed

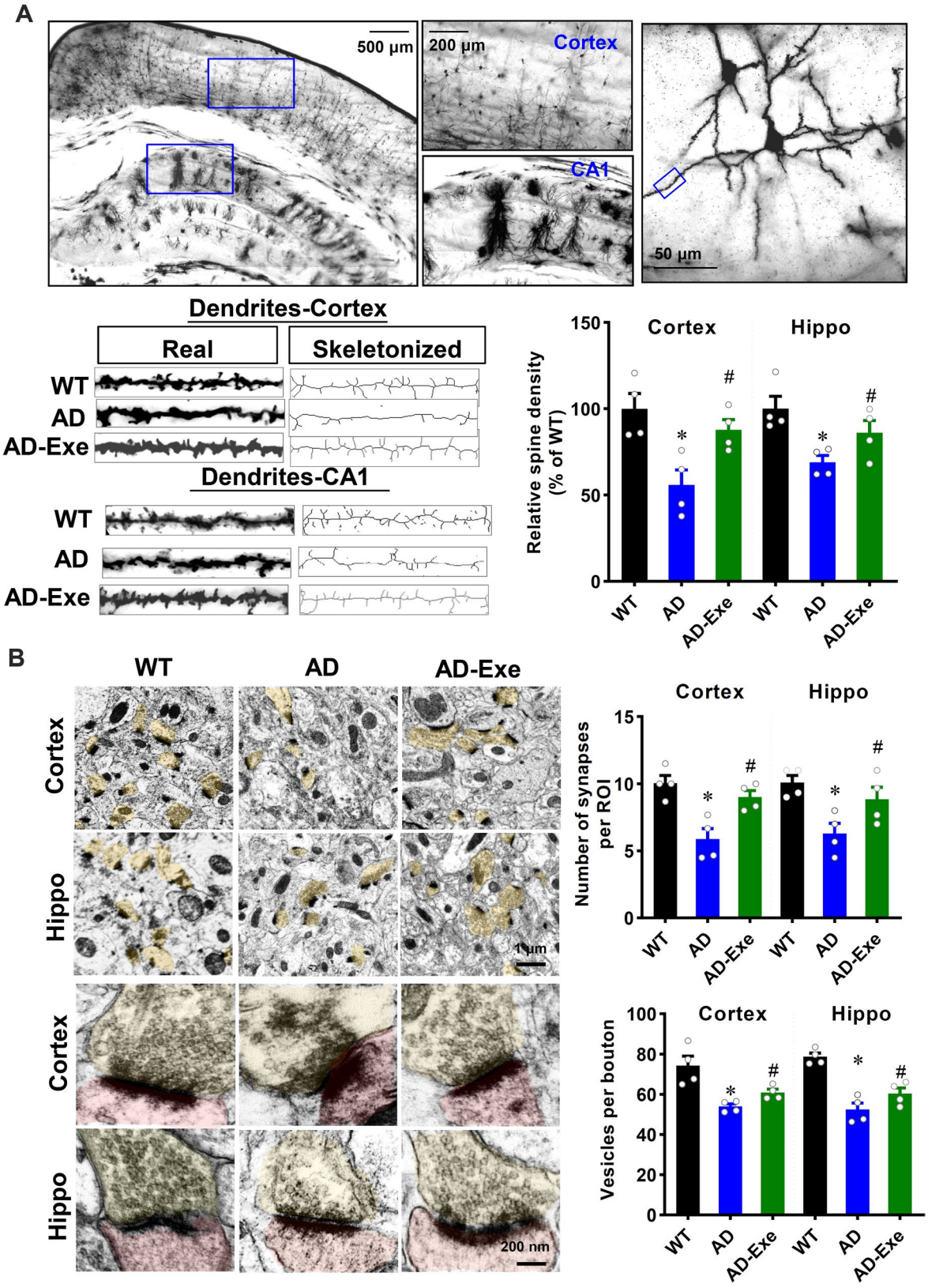
A
500 μm
200 μm
Cortex
CA1
50 μm
Dendrites-Cortex
Real
Skeletonized
WT
AD
AD-Exe
Dendrites-CA1
WT
AD
AD-Exe
Relative spine density (% of WT)
150
100
50
0
Cortex
Hippo
*
#
WT
AD
AD-Exe
B
WT
AD
AD-Exe
Cortex
Hippo
1 μm
200 nm
Number of synapses per ROI
15
10
5
0
Vesicles per bouton
100
80
60
40
20
0

◂**Fig. 3** Long-term exercise training preserves dendritic spine density, synapses, and synaptic vesicles of TgF344-AD rats. **A** Representative images of Golgi staining of cortex and hippocampus. Selected dendritic segments from the cortex and hippocampus were skeletonized using ImageJ software and analyzed. **B** Representative images of synapses in cortex and hippocampus. The numbers of synapses and synaptic vesicles per pre-synaptic bouton were counted and analyzed. All data are expressed as mean ± SEM ($n = 4$). $^{*}P < 0.05$ versus WT group, $^{\#}P < 0.05$ versus AD group

robustly decreased MAP2 fluorescent intensity compared with WT animals, and this decrease could be significantly alleviated by long-term exercise pretreatment. Furthermore, MBP, a major protein of the myelin sheath of a neuron, was measured in both the cortex and hippocampus. As shown in Fig. 4B, AD animals exhibited a significantly decreased MBP fluorescent intensity compared to WT animals. In contrast, long-term exercise pretreatment of AD animals alleviated this decrease, indicating that exercise training protects against damage to the myelin sheath of neurons. TUNEL staining was performed to determine whether long-term exercise training could inhibit neuronal apoptosis. As presented in Fig. 4C, neuronal apoptosis was detected in AD animals by the presence of a markedly increased number of TUNEL-positive cells in the cortex and hippocampus. However, exercise treatment effectively decreased the number of TUNEL-positive cells, suggesting that long-term exercise training significantly repressed neuronal apoptosis in AD animals. Finally, Fluoro-Jade C staining was performed to assess neuronal degeneration. Results in Fig. 4D revealed that AD animals presented markedly increased neuronal degeneration, as evidenced by increased Fluoro-Jade C–positive cells as compared with WT animals. Intriguingly, long-term exercise treatment significantly attenuated neuronal degeneration in AD animals.

Long-term exercise training preserves mitochondrial dynamics and mitochondrial morphology in TgF344-AD rats

A healthy pool of mitochondria not only provides enough energy to support neuronal activity but also contributes to maintaining the oxidation–reduction reaction balance [1, 35]. Therefore, we next investigated the effects of long-term exercise on mitochondrial morphology and mitochondrial dynamics. As shown in Fig. 5A, representative confocal microscopy images of Tom20 staining were processed and analyzed by ImageJ software. Quantification of mitochondrial segments demonstrated a markedly higher degree of mitochondrial fragmentation in AD animals, as evidenced by increases in both total mitochondrial fragmentation and small particles and decreases in continuous mitochondrial structures. By contrast, the degree of mitochondrial fragmentation was dramatically alleviated by exercise pretreatment. In addition, the levels of the fusion protein MFN1 were significantly decreased in both the cortex and hippocampus of AD animals (AD vs. WT), which was alleviated by exercise pretreatment (Fig. 5B). Consistent with these results, the levels of Fis1, a well-known fission protein, were significantly increased in AD animals as compared with WT animals and long-term exercise animals (Fig. 5C). Taken together, these results indicate that long-term exercise pretreatment effectively alleviated excessive mitochondrial fragmentation in AD animals. Furthermore, representative electron microscopy images showed that AD animals displayed a damaged mitochondrial morphology, as evidenced by mitochondrial intima structure blurring and disturbed or missing mitochondrial crest in AD animals (Fig. 5D). However, the disruption of mitochondrial morphology was alleviated by long-term exercise pretreatment. PGC-1α stimulates mitochondrial biogenesis and contributes to the regulation of energy metabolism [36]. Western blotting analyses of PGC-1 in the cortex and hippocampus showed significantly decreased PGC-1 expression in AD animals compared to WT and exercise-treated AD animals (Fig. 5E), suggesting exercise pretreatment contributes to the regulation of mitochondrial biogenesis in TgF344-AD rats.

Long-term exercise training attenuates mitochondrial dysfunction-induced oxidative stress

Several lines of evidence suggest that brain tissue in AD patients is exposed to mitochondrial dysfunction–induced oxidative stress [1, 37, 38]. Therefore, we next investigated the effects of long-term exercise training pretreatment on oxidative stress. As shown in Fig. 6A, total antioxidant capacity was markedly decreased in AD animals (AD vs. WT). Notably, long-term exercise pretreatment significantly attenuated this decrease, suggesting that long-term exercise

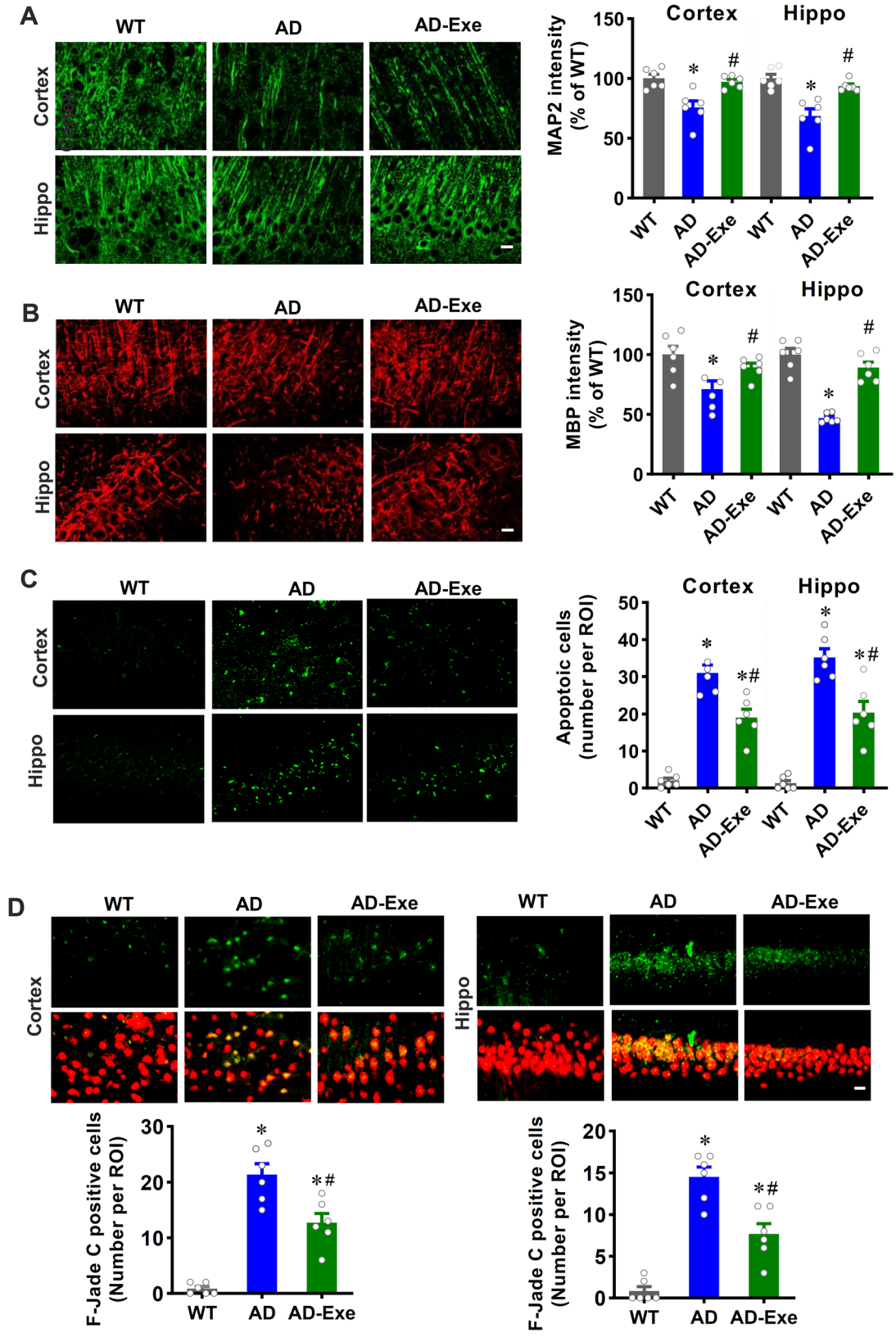
A
WT
AD
AD-Exe
Cortex
Hippo
MAP2 intensity (% of WT)
Cortex
Hippo
B
MBP intensity (% of WT)
C
Apoptoic cells (number per ROI)
D
F-Jade C positive cells (Number per ROI)

◂**Fig. 4** Long-term exercise training alleviates neuronal damage, apoptosis, and degeneration in TgF344-AD rats. Representative confocal microscopy images of MAP2 (**A**) and MBP (**B**) taken from the cortex and hippocampus. The intensity of the immunoreactivity associated with MAP2 was quantified. **C** The number of apoptotic cells as measured by TUNEL staining. **D** Neuronal degeneration was assessed by F-Jade C staining. Scale bar = 10 μm. All data are expressed as mean ± SEM ($n = 6$). $^{*}P < 0.05$ versus WT group, $^{\#}P < 0.05$ versus AD group

training effectively preserved total antioxidant capacity in AD animals. Furthermore, the expression of the antioxidant enzyme SOD2 was determined using Western blotting analysis. Figure 6B reveals that the expression of SOD2 decreased in AD animals as compared to WT animals. In contrast, long-term exercise training prevented this reduction in both the cortex and hippocampus as compared to AD animals. The release of ROS was then detected by dihydroethidium (DHE) staining. As shown in Fig. 6C, AD animals displayed significantly increased ROS levels as compared with WT animals, which was markedly attenuated by long-term exercise pretreatment. Preservation of antioxidant capacity and SOD2 expression as well as alleviation of ROS production should correlate with reduced oxidative damage in the brain. Therefore, we next examined the effect of long-term exercise pretreatment on oxidative damage in the cortex and hippocampus. The results in Fig. 6D and E revealed that long-term exercise pretreatment did significantly reduce oxidative damage in the cortex and hippocampus of AD rats, as evidenced by decreased levels of lipid peroxidation product (MDA) and protein carbonyls. In addition, exercise pretreatment also decreased oxidative DNA damage, as evidenced by reduced 8-OHdG fluorescent intensity in AD animals receiving long-term exercise pretreatment.

Long-term exercise training alleviates gliosis and suppresses neuroinflammation in TgF344-AD rats

Reactive gliosis and neuroinflammation are closely associated with oxidative stress and contribute to the pathogenesis of Alzheimer's disease [3, 39]. We thus examined for the presence of gliosis by performing Iba-1 and GFAP fluorescent staining. As shown in Fig. 7A, the Iba-1 fluorescent intensity in both the cortex and hippocampus were significantly increased in AD animals as compared to that in WT animals, which was attenuated by long-term exercise pretreatment. Furthermore, we analyzed microglial morphology using ImageJ software and found decreased endpoints and process length in AD animals, and this effect was significantly alleviated by exercise pretreatment. In addition, as presented in Fig. 7B, representative fluorescent images of GFAP quantitative analyses demonstrated significantly increased GFAP intensity in AD animals, which was significantly ameliorated by long-term exercise training. Taken together, these results suggest that long-term exercise pretreatment strongly alleviates microglial overactivation and excessive astrogliosis in AD rats. Furthermore, inflammatory cytokine production was assessed by a rat cytokine array kit using protein samples from the rat cortex and hippocampus. As presented in Fig. 7C, a representative heat map depicting the changes of inflammatory cytokines across the various groups. Results in Fig. 7C revealed that the levels of pro-inflammatory cytokines including IL1-α, IL-1β, IL-3, IL-6, and TNF-α were significantly elevated in both the cortex and hippocampus of AD rats. In contrast, the increased levels of pro-inflammatory cytokines were markedly attenuated by long-term exercise pretreatment.

Discussion

In our previous study, using a novel rat AD model, we demonstrated exercise training alleviated the anxious-depressive–like behavior of transgenic AD rats in the early stages of AD pathogenesis [5]. In the current study, we investigated the effect of long-term exercise pretreatment on behavioral deficits and typical pathology in the late stage of AD. We demonstrated that (a) long-term exercise pretreatment alleviated memory impairment and anxious-depressive–like behavior of TgF344-AD rats at 18 months of age; (b) dendritic spine density and numbers of synaptic vesicles and synapses in both the cortex and hippocampus were preserved by long-term exercise pretreatment; (c) long-term exercise pretreatment alleviated Aβ deposition, tau hyperphosphorylation, neuronal degeneration, neuronal damage, and neuronal apoptosis; and (d) long-term exercise pretreatment preserved mitochondrial dynamics and mitochondrial morphology and attenuated mitochondrial dysfunction–related oxidative stress and neuroinflammation. These findings add to the growing body of evidence that

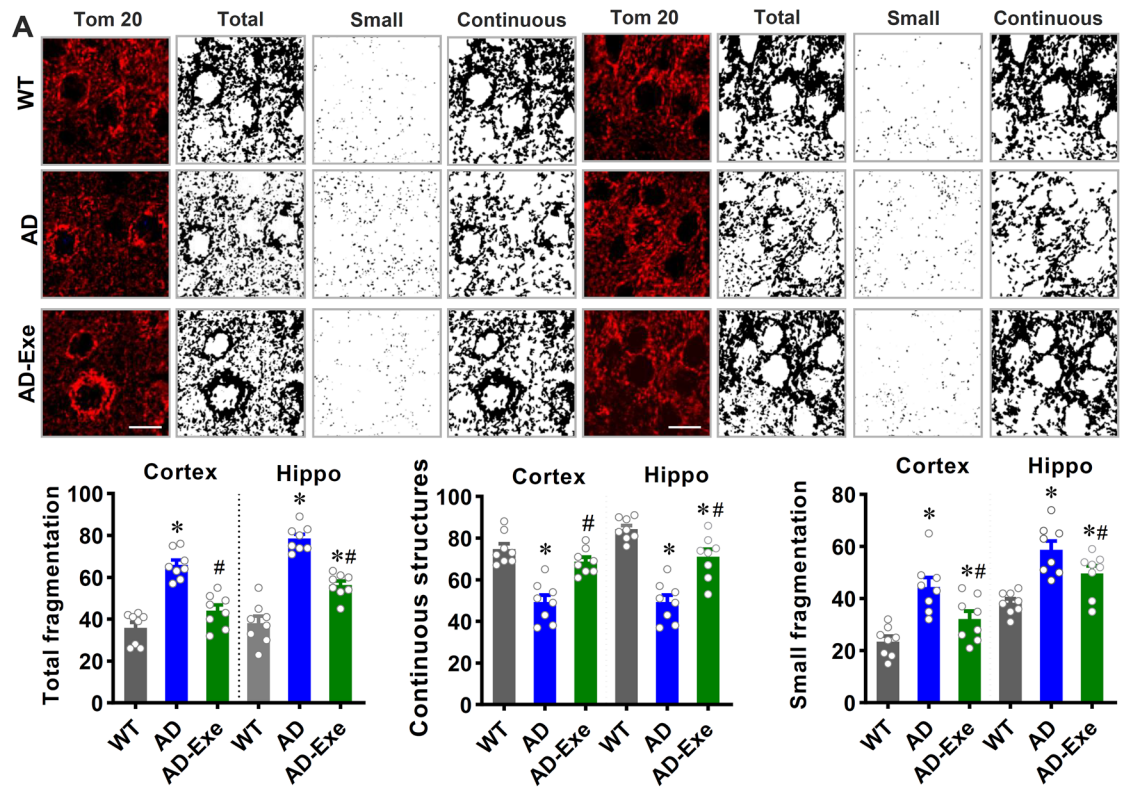
A
Tom 20
Total
Small
Continuous
WT
AD
AD-Exe
Cortex
Hippo
Total fragmentation
Continuous structures
Small fragmentation
B
Mfn1/DAPI
Releative intensity (% of WT)
AD
PBM
Mfn1
COX4
C
Releative intensity (% of WT)
Fis1
D
E
PGC-1α/DAPI
PGC-1α

◂**Fig. 5** Long-term exercise training preserves mitochondrial dynamics and mitochondrial morphology in TgF344-AD rats. **A** Representative confocal microscopy images of Tom20 staining captured from the cortex and hippocampus. Images of Tom20 fluorescent staining were further processed by ImageJ software into images with total particles, small particles (size < 1.5 μm), and continuous structure (size > 2 μm). $n = 8$. Scale bar = 10 μm. **B** Representative confocal microscopy images and Western blot results of MFN1 in the cortex and hippocampus. $n = 3$. **C** Western blot analysis of Fis1 ($n = 3$–4). **D** Representative transmission electron micrograph of mitochondria. Scale bar = 50 nm. **E** Representative confocal microscopy images and Western blot results of PGC-1α in the cortex and hippocampus ($n = 3$). Scale bar = 10 μm. Data are presented as mean ± SEM. $^{*}P < 0.05$ versus WT group, $^{\#}P < 0.05$ versus AD group

long-term exercise training is a potential approach to delay the progression of AD.

Although many long and expensive trials have been conducted, there are currently no effective pharmacotherapeutic methods approved for AD treatment [6]. The failure of clinical trials on AD has been proposed to be due to several reasons, including an inappropriate therapeutic time window, the wrong treatment target, and an inadequate understanding of the biopathology of Alzheimer's disease [6]. Experimental animal models of AD are indispensable tools better to understand pathogenesis and development of AD [11]. Currently, transgenic mice represent the most commonly used AD animal model; however, most mouse models only develop the accumulation of Aβ and often lack other typical pathological features of AD [10, 11, 40]. Therefore, the high clinical trial failure rate may be related to the premature translation of findings from animal models to human patients [10]. The physiological, pathological, and genetic characteristics of the TgF344-AD rat model used in the current study are more similar to AD patients as compared to mouse models [11, 12]. The TgF344-AD rat model can mirror all of the characteristic hallmarks of AD pathology in humans [11]. Consistent with previous studies [5, 12], our study demonstrated the presence of amyloid plaques and PHF in the TgF-344 AD rat model, which were significantly ameliorated by long-term exercise pretreatment. In addition, rats are 4–5 million years closer to humans in evolution than mice and have a richer and more complex behavioral phenotype [5, 12]. Therefore, we used this transgenic AD rat model to study the effects of exercise on learning, memory, and anxious-depressive–like behavior. In the current study, 18-month-old AD animals displayed learning and memory deficits and anxious-depressive–like behavior, which were also alleviated by long-term exercise pretreatment. Taken together, our findings support the beneficial role of long-term exercise training on the alleviation of learning and memory deficits and anxious-depressive–like behavior in AD.

Various types of exercise training have been studied in neurodegenerative diseases, including forced and voluntary exercise [3, 5, 41]. In our study, treadmill exercise was applied as an exercise intervention in AD. However, different from voluntary exercise training, forced exercise intervention may increase the stress response. Therefore, following our previous studies, an adaptive training stage that gradually increases in speed and intensity was included in the exercise paradigm to minimize the stress [5, 42]. Consistent with previous studies, we found the beneficial effects of forced exercise training in attenuating cognitive deficits and neuropathology [3, 42]. Unlike previous studies, our study focuses on using long-term exercise as an early lifestyle intervention to reduce AD pathology in a novel rat model of AD [42]. We demonstrated that early exercise intervention, even if followed in "middle age" by a sedentary lifestyle, can still have significant and lasting effects in preventing hallmark pathologies associated with AD. These results indicate that healthy people or AD patients with cognitive decline may still benefit from early exercise intervention, even though they cannot maintain exercise training in later life because of movement deficits caused by AD pathology or other diseases. The exercise paradigm in our study was an aerobic exercise performed three times a week—an exercise intervention that is feasible for patients with mild AD to perform [43]. Furthermore, the exercise paradigm used in our study is consistent with the exercise paradigm suggested by a previous clinical trial of exercise in patients with cognitive decline [43]. In the clinical trial, people who exercise three to five times per week had a significantly lower risk of AD than those living a sedentary lifestyle or exercising less than three times per week [43]. Although more studies are still needed, we believe long-term voluntary exercise can also have a beneficial effect in slowing down AD pathology because a previous study found that forced and voluntary exercises almost equally reverse behavioral deficits in experimental AD models [44].

Dendritic spine loss occurs in both the cortex and hippocampus and displays a stronger correlation to cognitive decline than neuronal loss and neurofibrillary

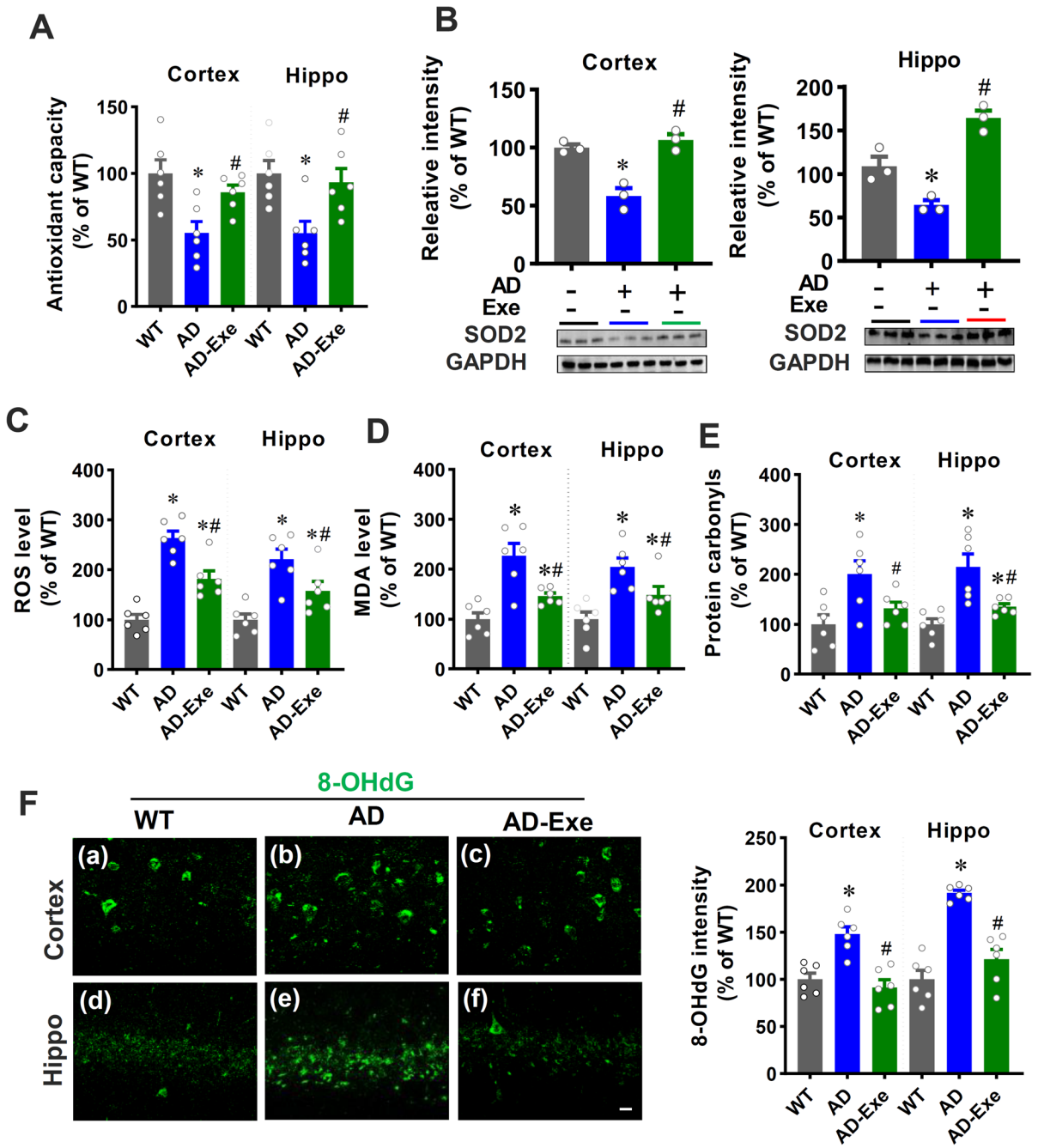

Fig. 6 Long-term exercise training attenuates mitochondrial dysfunction-induced oxidative stress. **A** Total antioxidative capacity ($n=6$). **B** Western blot results of SOD2 in cortex and hippocampus ($n=3$). **C** ROS level, **D** MDA level, and **E** protein carbonyl levels in the cortex and hippocampus were measured using related assay kits ($n=6$). **F** Oxidized DNA damage was measured by 8-OHdG staining ($n=6$). Scale bar = 10 μm. Data are presented as mean ± SEM. $^{*}P<0.05$ versus WT group, $^{\#}P<0.05$ versus AD group

tangles in AD [45–47]. Our findings, accordingly, revealed a significant decrease of dendritic spines in the cortex and hippocampus of AD rats. Notably, long-term exercise training markedly alleviated the dendritic spines loss in AD. Furthermore, according to a previous study, AD patients also display a significant loss of synapses compared with healthy individuals [47]. AD patients, even at the early stages of the disease, had significantly fewer synapses [48]. Our previous findings showed a loss of the presynaptic marker synaptophysin and postsynaptic marker spinophilin in a sporadic Alzheimer's rat model [3]. Consistent with these findings, our study revealed a significant loss of synapses in both cortex and hippocampus of transgenic AD rats. Interestingly, long-term exercise pretreatment was able to preserve the number of synapses. Furthermore, a previous study found decreased presynaptic vesicles in the AD mouse model [49]. In the current study, we also found reduced presynaptic vesicles in TgF-344 AD rats. Intriguing, long-term exercise training was able to preserve the presynaptic vesicle stores.

According to previous studies, the Aβ-overproducing Tg AD mouse model cannot display a robust neuronal loss without additional human transgenes that are not related to familial AD [12, 50, 51]. However, our current study confirmed the extensive neuronal loss in both cortex and hippocampus in TgF344-AD rats. Importantly, long-term exercise training significantly reduced neuronal apoptosis and neuronal degeneration in TgF344-AD rats. In addition, we also measured the effect of long-term exercise training on neuronal damage. Using neuronal damage-sensitive markers, our study revealed markedly increased neuronal damage in the cortex and hippocampus of AD rats, which was significantly ameliorated by exercise pretreatment. Taken together, these results demonstrated the beneficial role of long-term exercise pretreatment in neuronal protection.

Our study also revealed an important effect of long-term exercise training on preserving mitochondrial dynamics and mitochondrial morphology in AD rats. The pivotal role of mitochondria in AD has been widely accepted, and mitochondrial dysfunction has been recognized as a major contributing factor in the development of AD [1, 52]. Mitochondrial dynamic imbalance in AD induces a shift from mitochondrial fusion toward mitochondria fission, causing excessive mitochondrial fragmentation [1, 53, 54]. Consistent with earlier research, we found an imbalance of mitochondrial dynamics, with excessive mitochondrial fragmentation and decreased expression of fusion-related proteins in AD rats. Notably, long-term exercise pretreatment preserved mitochondrial dynamics and mitochondrial morphology in AD rats. Damage to mitochondrial morphology and mitochondrial function leads to excessive ROS production and induces oxidative stress [1, 55]. In agreement with these findings, our study demonstrated decreased total antioxidant capacity, decreased expression of the key antioxidative enzyme SOD2, and elevated ROS production in both the cortex and hippocampus of AD animals. Furthermore, excessive ROS production resulted in oxidative damage to lipid, protein, and DNA, as evidenced by increased lipid peroxidation, protein carbonyls, and oxidative modifications of DNA. Importantly, long-term exercise pretreatment was able to attenuate oxidative stress and oxidative damage to lipid, protein, and DNA.

Finally, our study also revealed an anti-inflammatory effect of long-term exercise pretreatment. In AD, neuroinflammation, mitochondrial dysfunction, and oxidative stress induce a vicious cycle and contribute to the development of AD [56–58]. Inflammatory cytokines released from activated microglia and astrocytes trigger cellular mitochondrial metabolism changes that result in excessive release of ROS, as well as inhibition of mitochondrial oxidative phosphorylation and ATP production [1, 57, 59]. The excessive ROS production induces increased mitochondrial membrane permeabilization and altered mitochondrial dynamics [1, 57, 60]. Thereafter, the fragmented mitochondria further propagate neuroinflammation in neurodegenerative disease [61]. Therefore, neuroinflammation also plays a crucial role in AD [56]. In the present study, AD animals displayed activated microglia with enlarged soma and retracted and shortened processes. GFAP immunostaining results also demonstrated activated astrocyte with an increase in GFAP intensity and robust enlargement of astrocyte size. Interestingly, long-term exercise training was able to attenuate the activation of microglia and astrocytes. Furthermore, the increased pro-inflammatory cytokine release was alleviated by long-term exercise training.

Conclusions

In summary, our study demonstrates long-term exercise training can ameliorate learning and memory

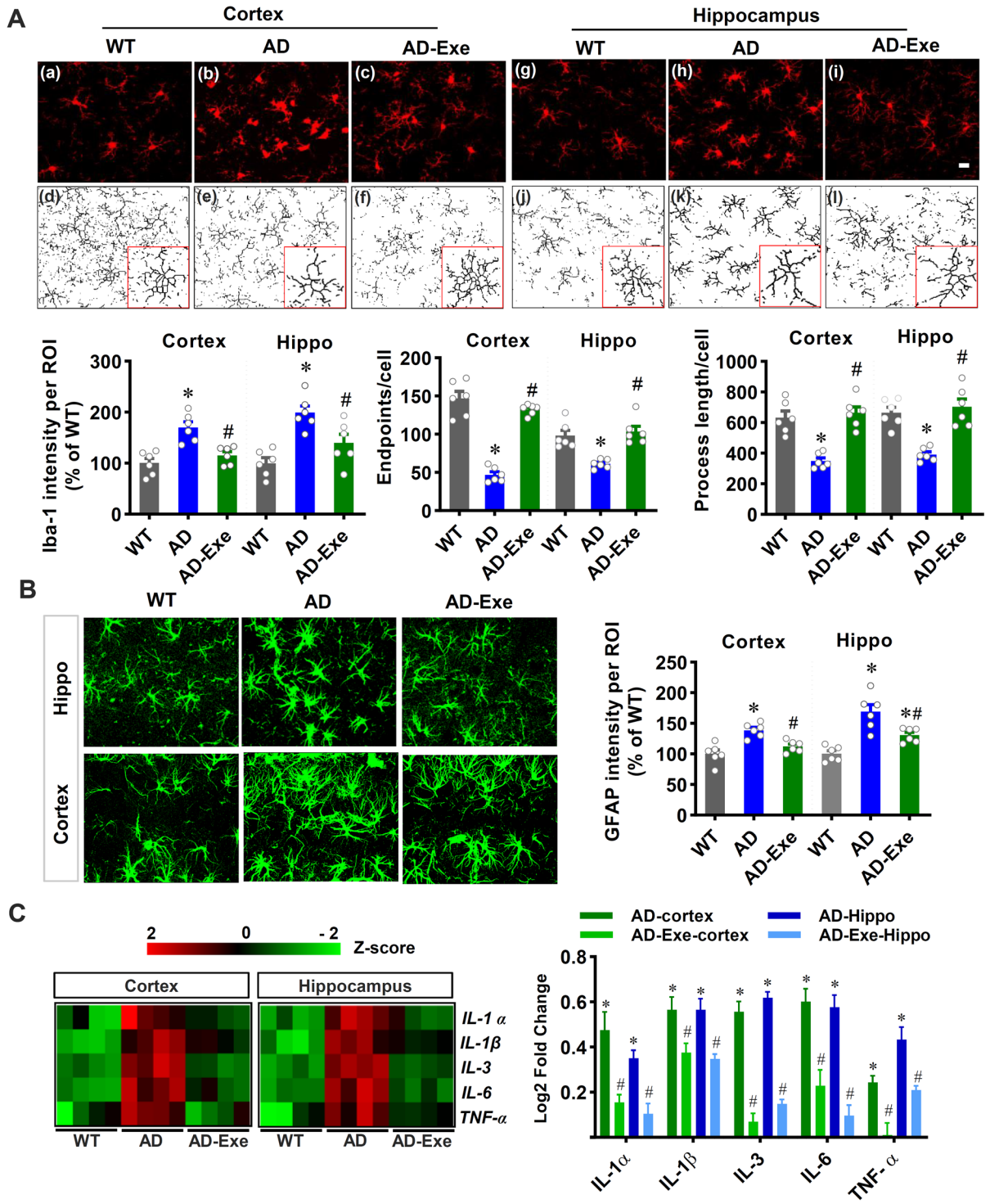

deficits and anxious-depressive–like behavior of AD rats. Importantly, we also found long-term exercise training could alleviate the accumulation of Aβ and tau hyperphosphorylation. The protective effect of long-term exercise training was also demonstrated by the preservation of synapses and mitochondrial

◂**Fig. 7** Long-term exercise training alleviates gliosis and suppresses neuroinflammation in TgF344-AD rats. **A** Representative confocal microscopy images of Iba-1 staining in the cortex and hippocampus. The microscopy images of Iba-1 were processed and analyzed by ImageJ software. Iba-1 intensity, endpoints, and processes per cell were analyzed. **B** The astrocyte marker GFAP was stained for the measurement of astrocyte activation. GFAP fluorescent intensity was analyzed. **C** Pro-inflammatory cytokines were measured in both the cortex and hippocampus using a rat cytokine array kit. Acquired values were transformed into *z*-scores and presented as a heat map for a better view. Log2 fold changes were calculated compared with the WT group. The Log2 fold changes of WT is zero and did not shown in the graph. Data are presented as mean ± SEM ($n = 4–6$). $^{*}P < 0.05$ versus WT group, $^{\#}P < 0.05$ versus AD group

morphology, reduced oxidative stress, and the suppression of gliosis and neuroinflammation. Taken together, using a novel AD rat model to better mimic the pathology of AD patients, our findings provide more evidence supporting the beneficial effects of long-term exercise training on familial AD. Future work should further investigate the mechanisms underlying this preventative effect and determine how long these beneficial effects can last after terminating the exercise pretreatment.

Funding This research was supported by a grant from the National Institute of Aging, National Institutes of Health (1RF1AG058603).

Declarations

Ethics approval Animal environment, housing, management, and other procedures were approved by our Institutional Animal Care and Use Committee (IACUC) of Augusta University and complied with National Institutes of Health guidelines.

Competing interests The authors declare no competing interests.

References

1. Yang L, Youngblood H, Wu C, Zhang Q. Mitochondria as a target for neuroprotection: role of methylene blue and photobiomodulation. Transl Neurodegener. 2020;9:19.
2. Gallardo G, Holtzman DM. Amyloid-beta and tau at the crossroads of Alzheimer's disease. Adv Exp Med Biol. 2019;1184:187–203.
3. Wu C, Yang L, Tucker D, Dong Y, Zhu L, Duan R, Liu TC, Zhang Q. Beneficial effects of exercise pretreatment in a sporadic Alzheimer's Rat model. Med Sci Sports Exerc. 2018;50:945–56.
4. 2020 Alzheimer's disease facts and figures. Alzheimers Dement 2020.
5. Wu C, Yang L, Li Y, Dong Y, Yang B, Tucker LD, Zong X, Zhang Q. Effects of exercise training on anxious-depressive-like behavior in Alzheimer Rat. Med Sci Sports Exerc. 2020;52:1456–69.
6. Yiannopoulou KG, Anastasiou AI, Zachariou V, Pelidou SH: Reasons for failed trials of disease-modifying treatments for Alzheimer disease and their contribution in recent research. Biomedicines 2019. 7.
7. Kametani F, Hasegawa M. Reconsideration of amyloid hypothesis and Tau hypothesis in Alzheimer's disease. Front Neurosci. 2018;12:25.
8. Gong CX, Liu F, Iqbal K. Multifactorial hypothesis and multi-targets for Alzheimer's disease. J Alzheimers Dis. 2018;64:S107–17.
9. Iqbal K, Grundke-Iqbal I. Alzheimer's disease, a multifactorial disorder seeking multitherapies. Alzheimers Dement. 2010;6:420–4.
10. Gotz J, Bodea LG, Goedert M. Rodent models for Alzheimer disease. Nat Rev Neurosci. 2018;19:583–98.
11. Drummond E, Wisniewski T. Alzheimer's disease: experimental models and reality. Acta Neuropathol. 2017;133:155–75.
12. Cohen RM, Rezai-Zadeh K, Weitz TM, Rentsendorj A, Gate D, Spivak I, Bholat Y, Vasilevko V, Glabe CG, Breunig JJ, et al. A transgenic Alzheimer rat with plaques, tau pathology, behavioral impairment, oligomeric abeta, and frank neuronal loss. J Neurosci. 2013;33:6245–56.
13. Stanciu GD, Luca A, Rusu RN, Bild V, Beschea Chiriac SI, Solcan C, Bild W, Ababei DC: Alzheimer's disease pharmacotherapy in relation to cholinergic system involvement. Biomolecules 2019. 10.
14. Fricker M, Tolkovsky AM, Borutaite V, Coleman M, Brown GC. Neuronal cell death. Physiol Rev. 2018;98:813–80.
15. Barage SH, Sonawane KD. Amyloid cascade hypothesis: pathogenesis and therapeutic strategies in Alzheimer's disease. Neuropeptides. 2015;52:1–18.
16. Niikura T, Tajima H, Kita Y. Neuronal cell death in Alzheimer's disease and a neuroprotective factor, humanin. Curr Neuropharmacol. 2006;4:139–47.
17. Perneczky R. Dementia treatment versus prevention. Dialogues Clin Neurosci. 2019;21:43–51.
18. Kashyap G, Bapat D, Das D, Gowaikar R, Amritkar RE, Rangarajan G, Ravindranath V, Ambika G. Synapse loss and progress of Alzheimer's disease -a network model. Sci Rep. 2019;9:6555.
19. Mendiola-Precoma J, Berumen LC, Padilla K, Garcia-Alcocer G. Therapies for prevention and treatment of Alzheimer's disease. Biomed Res Int. 2016;2016:2589276.
20. Zhang J, Tucker LD. DongYan, Lu Y, Yang L, Wu C, Li Y, Zhang Q: Tert-butylhydroquinone post-treatment attenuates neonatal hypoxic-ischemic brain damage in rats. Neurochem Int. 2018;116:1–12.
21. Eagle AL, Wang H, Robison AJ: Sensitive assessment of hippocampal learning using temporally dissociated passive avoidance task. Bio-protocol 2016. 6.

22. Shoji H, Takao K, Hattori S, Miyakawa T: Contextual and cued fear conditioning test using a video analyzing system in mice. Journal of visualized experiments : JoVE 2014.
23. Walf AA, Frye CA. The use of the elevated plus maze as an assay of anxiety-related behavior in rodents. Nat Protoc. 2007;2:322–8.
24. Kraeuter AK, Guest PC, Sarnyai Z. The open field test for measuring locomotor activity and anxiety-like behavior. Methods Mol Biol. 2019;1916:99–103.
25. Duca FA, Swartz TD, Covasa M. Effect of diet on preference and intake of sucrose in obese prone and resistant rats. PloS one. 2014;9:e111232.
26. Yang L, Dong Y, Wu C, Youngblood H, Li Y, Zong X, Li L, Xu T, Zhang Q. Effects of prenatal photobiomodulation treatment on neonatal hypoxic ischemia in rat offspring. Theranostics. 2021;11:1269–94.
27. Zong X, Dong Y, Li Y, Yang L, Li Y, Yang B, Tucker L, Zhao N, Brann DW, Yan X, et al. Beneficial effects of theta-burst transcranial magnetic stimulation on stroke injury via improving neuronal microenvironment and mitochondrial integrity. Transl Stroke Res. 2020;11:450–67.
28. Tucker LD, Lu Y, Dong Y, Yang L, Li Y, Zhao N, Zhang Q. Photobiomodulation therapy attenuates hypoxic-ischemic injury in a neonatal Rat model. Journal of molecular neuroscience : MN. 2018;65:514–26.
29. Yang L, Dong Y, Wu C, Li Y, Guo Y, Yang B, Zong X, Hamblin MR, Liu TC, Zhang Q. Photobiomodulation preconditioning prevents cognitive impairment in a neonatal rat model of hypoxia-ischemia. Journal of biophotonics. 2019;12:e201800359.
30. Young K, Morrison H: Quantifying microglia morphology from photomicrographs of immunohistochemistry prepared tissue using ImageJ. Journal of visualized experiments : JoVE 2018.
31. Sun L, Li FH, Li T, Min Z, Yang LD, Gao HE, Wu DS, Xie T. Effects of high-intensity interval training on adipose tissue lipolysis, inflammation, and metabolomics in aged rats. Pflugers Arch. 2020;472:245–58.
32. Yang L, Tucker D, Dong Y, Wu C, Lu Y, Li Y, Zhang J, Liu TC, Zhang Q. Photobiomodulation therapy promotes neurogenesis by improving post-stroke local microenvironment and stimulating neuroprogenitor cells. Exp Neurol. 2018;299:86–96.
33. Rajmohan R, Reddy PH. Amyloid-beta and phosphorylated tau accumulations cause abnormalities at synapses of Alzheimer's disease neurons. J Alzheimers Dis. 2017;57:975–99.
34. Johnson GV, Stoothoff WH. Tau phosphorylation in neuronal cell function and dysfunction. J Cell Sci. 2004;117:5721–9.
35. Wang W, Zhao F, Ma X, Perry G, Zhu X. Mitochondria dysfunction in the pathogenesis of Alzheimer's disease: recent advances. Mol Neurodegener. 2020;15:30.
36. Liang H, Ward WF. PGC-1alpha: a key regulator of energy metabolism. Adv Physiol Educ. 2006;30:145–51.
37. Sharma A, Liaw K, Sharma R, Zhang Z, Kannan S, Kannan RM. Targeting mitochondrial dysfunction and oxidative stress in activated microglia using dendrimer-based therapeutics. Theranostics. 2018;8:5529–47.
38. Wang X, Wang W, Li L, Perry G, Lee HG, Zhu X. Oxidative stress and mitochondrial dysfunction in Alzheimer's disease. Biochem Biophys Acta. 2014;1842:1240–7.
39. Heneka MT, Carson MJ, El Khoury J, Landreth GE, Brosseron F, Feinstein DL, Jacobs AH, Wyss-Coray T, Vitorica J, Ransohoff RM, et al. Neuroinflammation in Alzheimer's disease. The Lancet Neurology. 2015;14:388–405.
40. Neff EP. Animal models of Alzheimer's disease embrace diversity. Lab Anim. 2019;48:255–9.
41. Richter H, Ambree O, Lewejohann L, Herring A, Keyvani K, Paulus W, Palme R, Touma C, Schabitz WR, Sachser N. Wheel-running in a transgenic mouse model of Alzheimer's disease: protection or symptom? Behav Brain Res. 2008;190:74–84.
42. Lu Y, Dong Y, Tucker D, Wang R, Ahmed ME, Brann D, Zhang Q. Treadmill exercise exerts neuroprotection and regulates microglial polarization and oxidative stress in a streptozotocin-induced Rat model of sporadic Alzheimer's disease. J Alzheimers Dis. 2017;56:1469–84.
43. Frederiksen KS, Sobol N, Beyer N, Hasselbalch S, Waldemar G. Moderate-to-high intensity aerobic exercise in patients with mild to moderate Alzheimer's disease: a pilot study. Int J Geriatr Psychiatry. 2014;29:1242–8.
44. Belviranli M, Okudan N. Voluntary, involuntary and forced exercises almost equally reverse behavioral impairment by regulating hippocampal neurotrophic factors and oxidative stress in experimental Alzheimer's disease model. Behav Brain Res. 2019;364:245–55.
45. Penzes P, Cahill ME, Jones KA, VanLeeuwen JE, Woolfrey KM. Dendritic spine pathology in neuropsychiatric disorders. Nat Neurosci. 2011;14:285–93.
46. Walsh DM, Selkoe DJ. Deciphering the molecular basis of memory failure in Alzheimer's disease. Neuron. 2004;44:181–93.
47. DeKosky ST, Scheff SW. Synapse loss in frontal cortex biopsies in Alzheimer's disease: correlation with cognitive severity. Ann Neurol. 1990;27:457–64.
48. Dorostkar MM, Zou C, Blazquez-Llorca L, Herms J. Analyzing dendritic spine pathology in Alzheimer's disease: problems and opportunities. Acta Neuropathol. 2015;130:1–19.
49. Chakroborty S, Hill ES, Christian DT, Helfrich R, Riley S, Schneider C, Kapecki N, Mustaly-Kalimi S, Seiler FA, Peterson DA, et al. Reduced presynaptic vesicle stores mediate cellular and network plasticity defects in an early-stage mouse model of Alzheimer's disease. Mol Neurodegener. 2019;14:7.
50. Colton CA, Wilcock DM, Wink DA, Davis J, Van Nostrand WE, Vitek MP. The effects of NOS2 gene deletion on mice expressing mutated human AbetaPP. J Alzheimers Dis. 2008;15:571–87.
51. Wilcock DM, Lewis MR, Van Nostrand WE, Davis J, Previti ML, Gharkholonarehe N, Vitek MP, Colton CA. Progression of amyloid pathology to Alzheimer's disease pathology in an amyloid precursor protein transgenic mouse model by removal of nitric oxide synthase 2. J Neurosci. 2008;28:1537–45.
52. Perez Ortiz JM, Swerdlow RH. Mitochondrial dysfunction in Alzheimer's disease: role in pathogenesis

and novel therapeutic opportunities. Br J Pharmacol. 2019;176:3489–507.
53. Zhang L, Zhang Y, Chang X, Zhang X. Imbalance in mitochondrial dynamics induced by low PGC-1alpha expression contributes to hepatocyte EMT and liver fibrosis. Cell Death Dis. 2020;11:226.
54. Zhu X, Perry G, Smith MA, Wang X. Abnormal mitochondrial dynamics in the pathogenesis of Alzheimer's disease. J Alzheimers Dis. 2013;33(Suppl 1):S253-262.
55. Guo C, Sun L, Chen X, Zhang D. Oxidative stress, mitochondrial damage and neurodegenerative diseases. Neural Regen Res. 2013;8:2003–14.
56. Kinney JW, Bemiller SM, Murtishaw AS, Leisgang AM, Salazar AM, Lamb BT. Inflammation as a central mechanism in Alzheimer's disease. Alzheimers Dement (N Y). 2018;4:575–90.
57. van Horssen J, van Schaik P, Witte M. Inflammation and mitochondrial dysfunction: a vicious circle in neurodegenerative disorders? Neuroscience letters. 2019;710:132931.
58. Hensley K. Neuroinflammation in Alzheimer's disease: mechanisms, pathologic consequences, and potential for therapeutic manipulation. J Alzheimers Dis. 2010;21:1–14.
59. Galasko D, Montine TJ. Biomarkers of oxidative damage and inflammation in Alzheimer's disease. Biomark Med. 2010;4:27–36.
60. Retta SF, Chiarugi P, Trabalzini L, Pinton P, Belkin AM. Reactive oxygen species: friends and foes of signal transduction. Journal of signal transduction. 2012;2012:534029.
61. Joshi AU, Minhas PS, Liddelow SA, Haileselassie B, Andreasson KI, Dorn GW 2nd, Mochly-Rosen D. Fragmented mitochondria released from microglia trigger A1 astrocytic response and propagate inflammatory neurodegeneration. Nat Neurosci. 2019;22:1635–48.